Published in final edited form as:
Genes Chromosomes Cancer. 2009 October ; 48(10): 865–885. doi:10.1002/gcc.20692.

Identifying the Molecular Signature of the Interstitial Deletion 7q Subgroup of Uterine Leiomyomata Using a Paired Analysis

Jennelle C. Hodge[1,2,3], **Peter J. Park**[2,4,5], **Jonathan M. Dreyfuss**[4], **Iman Assil-Kishawi**[6], **Priya Somasundaram**[1], **Luwam G. Semere**[7], **Bradley J. Quade**[2,8], **Allison M. Lynch**[1], **Elizabeth A. Stewart**[1,2], and **Cynthia C. Morton**[1,2,4,8,*]

[1]Department of Obstetrics, Gynecology and Reproductive Biology, Brigham and Women's Hospital, Boston, 02115, USA

[2]Harvard Medical School, Boston, 02115, USA

[3]Department of Laboratory Medicine and Pathology, Mayo Clinic, Rochester, 55905, USA

[4]Harvard-Partners Center for Genetics and Genomics, Boston, 02115, USA

[5]Children's Hospital Informatics Program, Boston, 02115, USA

[6]Agilent Technologies, Inc., Santa Clara, 95051, USA

[7]Division of Health Sciences and Technology, Harvard University-Massachusetts Institute of Technology, Cambridge, 02139, USA

[8]Department of Pathology, Brigham and Women's Hospital, Boston, 02115, USA

Abstract

Uterine leiomyomata (UL), the most common neoplasm in reproductive-age women, have recurrent cytogenetic abnormalities including del(7)(q22q32). To develop a molecular signature, matched del(7q) and non-del(7q) tumors identified by FISH or karyotyping from 11 women were profiled with expression arrays. Our analysis using paired t-tests demonstrates this matched design is critical to eliminate confounding effects of genotype and environment that underlie patient variation. A gene list ordered by genome-wide significance showed enrichment for the 7q22 target region. Modification of the gene list by weighting each sample for percent of del(7q) cells to account for the mosaic nature of these tumors further enhanced the frequency of 7q22 genes. Pathway analysis revealed two of the 19 significant functional networks were associated with development and the most represented pathway was protein ubiquitination, which can influence tumor development by stabilizing oncoproteins and destabilizing tumor suppressor proteins. Array CGH (aCGH) studies determined the only consistent genomic imbalance was deletion of 9.5 megabases from 7q22-7q31.1. Combining the aCGH data with the del(7q) UL mosacism-weighted expression analysis resulted in a list of genes that are commonly deleted and whose copy number is correlated with significantly decreased expression. These genes include the proliferation inhibitor *HPB1*, the loss of expression of which has been associated with invasive breast cancer, as well as the mitosis integrity-maintenance tumor suppressor *RINT1*. This study provides a molecular signature of the del(7q) UL subgroup and will serve as a platform for future studies of tumor pathogenesis.

*Correspondence to: Cynthia C. Morton, Ph.D., 77 Avenue Louis Pasteur, New Research Building Room 160, Boston, MA 02115, Phone: 617-525-4535, Fax: 617-525-4533, Email: cmorton@partners.org.

Keywords

uterine leiomyomata; fibroids; del(7)(q22q32); expression; microarray

INTRODUCTION

Uterine leiomyomata (UL) are tumors commonly referred to as fibroids that arise from the uterine smooth muscle wall. Despite their non-malignant nature, UL represent a major concern in women's health through their induction of significant morbidity in many of the approximately 25% of reproductive-age women in whom they are clinically detected (Buttram and Reiter, 1981). The overall prevalence is even higher, as systematic histological examination of hysterectomy specimens identified UL in approximately 77% of women (Cramer and Patel, 1990). This frequency, and symptoms including bladder dysfunction, abdominal pain, excessive menstrual bleeding and impaired fertility (Rein and Nowak, 1992; Coronado et al., 2000), leads UL to be the primary indication for hysterectomy and account for approximately 1 in 5 visits to a gynecologist, thereby resulting in expenditures of greater than 2.1 billion health care dollars annually in the U.S. (Lepine et al., 1997; Flynn et al., 2006; Hartmann et al., 2006).

Approximately 40% of UL have cytogenetic alterations including simple and recurrent deletions, inversions and translocations (Nibert and Heim, 1990; Meloni et al., 1992). These abnormalities were used to classify UL into subgroups and provide landmarks for gene discovery. One of the largest UL subgroups is defined by the presence of chromosome 7 long arm abnormalities, most commonly the interstitial deletion del(7)(q22q32), which represents approximately 15% of all UL and 20–35% of karyotypically abnormal UL (Nibert and Heim, 1990; Ozisik et al., 1993; Sargent et al., 1994; Xing et al., 1997). Deletion of 7q can sometimes be found as the sole alteration in a non-mosaic state, suggesting that it may play a primary early role in UL pathobiology.

Defining the del(7q) pathogenetic region has proven challenging. Initial work with rare translocations identified the gene-rich band 7q22 as the minimal cytogenetic region of importance (Ozisik et al., 1993; Sargent et al., 1994). Further refinement was attempted by multiple groups through loss of heterozygosity (LOH) analysis using polymorphic microsatellite markers; however, conflicting minimally deleted regions and inconsistent LOH maps have resulted. The most consistent common region of overlap based on the March 2006 assembly of the UCSC genome browser as defined by five previous studies is located between markers *D7S2453* and *D7S501* in 7q22.2-q22.3 (Zeng et al., 1997; Sell et al., 1998; van der Heijden et al., 1998; Saito et al., 2005; Vanharanta et al., 2005). Additional regions were suggested as separate tumorigenic targets in del(7q) UL such as 7q31.1 and 7q34, but such results only reflect one sample in each study and lack independent confirmation (Ishwad et al., 1997; Sell et al., 2005; Vanharanta et al., 2007).

UL provide a unique model for tumor pathobiology investigation as on average six to seven neoplasms are present in an individual woman and each is clonal as demonstrated by analysis of repeat polymorphisms in the X-linked androgen receptor and phosphoglycerokinase genes (Cramer and Patel, 1990; Mashal et al., 1994; Hashimoto et al., 1995). In addition, UL are homogenous and often of a size to provide an abundant sample. We have taken advantage of this for expression profiling to compare directly UL with del(7q) and UL without del(7q) obtained concurrently from the same uterus.

As we will show, this matched (or paired) study design is critical in identifying genetic events associated with the del(7q) abnormality. This design has not been exploited by any

previous study and will nullify the confounding effect of patient to patient variability due to divergent genotype, environment, or interaction of genotype and environment.

MATERIALS AND METHODS

Clinical Material

GTG-banded karyotyping according to established protocols (Rein et al., 1991) or FISH (see below) were used to ascertain four UL with del(7q) (cases 1 to 4) and one UL that was mosaic for both del(7q) and t(12;14)(q15;q23-q24) (case 5) obtained from surgical specimens at Brigham and Women's Hospital (BWH) through a Partners HealthCare IRB-approved protocol. Using the same abnormality detection strategy, six UL with del(7q) (cases 6 to 11) were identified from an IRB-approved tissue bank of over 100 consented 25–50 year-old women who underwent myomectomy or hysterectomy at BWH. Participants consented for the tissue bank also completed detailed epidemiological surveys ascertaining clinical, reproductive, sexual, dietary, and family history. For each of these 11 cases, matched uterine myometrium and a non-del(7q) UL were obtained concurrently with the karyotypically abnormal UL. Each case was grossly confirmed to be a UL or myometrial specimen and when possible hematoxylin- and eosin-stained tissue sections underwent histologic evaluation.

Fluorescence *In Situ* Hybridization (FISH)

End-sequenced and FISH-verified bacterial artificial chromosomes (BACs) (Cheung et al., 2001) were selected using the University of California Santa Cruz Biotechnology Genome Browser and Database (http://genome.ucsc.edu) (Karolchik et al., 2003) and then obtained from the RP11 library (BACPAC Resource Center at the Children's Hospital Oakland Research Institute, Oakland, CA). DNA was isolated from bacterial cultures following a standard protocol consisting of alkaline lysis, neutralization and ethanol precipitation.

UL with del(7q) were identified by loss of probe RP11-374E17 at 7q22.2 with retention of the control probe RP11-71F18 at 7p21.1 by interphase FISH on nuclei from fresh fixed cell pellets as previously described (Moore et al., 2004). A total of 100 interphase nuclei were scored for each specimen. The probe set was validated on normal peripheral blood metaphases and on interphase nuclei from karyotype-confirmed del(7q) UL tumors. Each of the tumors was similarly screened by interphase FISH for another common chromosome abnormality in UL, t(12;14)(q15;q23-24), by assessing for the presence of a fusion signal of probes RP11-185D13 located at 12q15 and CTD-3225F7 at 14q24.

DNA Isolation

For the eight cases (2–3 and 6–11) for which tissue was available, a portion of each of the non-del(7q) UL and del(7q) UL was minced with scalpels and immediately placed in Buffer ATL (QIAGEN). Genomic DNA was isolated using the DNeasy Tissue kit with provided standard protocol (QIAGEN) and assessed for purity and quantity on a Nanodrop spectrophotometer (Thermo Scientific).

Array Comparative Genomic Hybridization (aCGH) Analysis

High quality genomic DNA from each of six cases (3, 6–9, and 11) was run on Agilent Human 244K CGH microarrays (Santa Clara, CA) using a standard direct method as described in the Agilent Oligonucleotide Array-Based CGH for Genomic DNA Analysis Protocol version 4.0 at www.chem.agilent.com. Briefly, DNA was restriction digested and each del(7q) UL (test sample) was labeled with Cy5 and each matched myometrium (control sample) was labeled with Cy3 using the Genomic DNA Labeling Kit PLUS (Agilent). The labeled DNA was then washed, yield quantified, and appropriate control and test samples

combined in equal amounts. After incubation in CotI DNA, blocking agent and hybridization buffer, each sample was applied to a 244K array to hybridize overnight followed by washing and array scanning. Data quality control measures were reviewed and array images created using Feature Extraction software v9.5 (Agilent). Data were imported into DNA Analytics software (Agilent) and analyzed for genomic copy number variation using the ADM2 algorithm with a 5.5 threshold, a 5 probe and ≥0.125 absolute log ratio filter, and fuzzy zero correction. The ADM2 algorithm gives a score that is proportional to the absolute log ratio within an interval and the number of probes that have a significantly different log ratio from that of the neighboring interval. The filter required that at least 5 consecutive probes had an absolute log ratio of ≥0.125 for an aberration to be called. The fuzzy zero correction took into account local and global data noise to reduce false positive calls. After establishing the aCGH-based DNA copy number aberrations, chromosome 7 data were aligned using the DNA Analytics software to the significantly expressed gene data ($P < 0.01$) from the del(7q) UL gene list weighted for percent of cells with the 7q deletion (the generation using Affymetrix arrays of which is described below).

RNA Isolation

A portion of each of the myometrial, non-del(7q) UL and del(7q) UL tissues in the 11 cases was frozen in liquid nitrogen immediately after surgical removal or placed directly into RNAlater solution (QIAGEN, Valencia, CA). RNA was isolated using the RNeasy Fibrous Tissue kit with provided standard protocol (QIAGEN) and assessed for purity and quantity on a Nanodrop spectrophotometer (Thermo Scientific, Wilmington, DE).

Quantitative Polymerase Chain Reaction (Q-PCR)

Total RNA from the del(7q) and non-del(7q) UL from each of four women (cases 4, 7, 10 and 11) was examined for *MLL5* gene expression. PCR was performed on the ABI PRISM 7900HT Sequence Detection System in a 384-well format. TaqMan Universal PCR MasterMix and a pre-designed and optimized Taqman Gene Expression Assay for quantitation of human *MLL5* RNA (Applied Biosystems, Foster City, CA) were used according to the manufacturer's instructions. Each RNA was run in quadruplicate and the Ct (cycle threshold) values of these replicates were averaged and then normalized by subtracting the Ct value of the co-amplified internal control housekeeping gene *GAPDH* for a ΔCt value. Data analysis used the comparative Ct method where the ΔCt of a non-del(7q) UL was used as a calibrator reference and subtracted from the ΔCt of the corresponding del(7q) UL to yield a ΔΔCt value. This was then converted into a fold-change relative to one using the following formula: *MLL5* expression = $2^{(-\Delta\Delta Ct)}$. This number was then averaged across the four samples.

Transcriptional Profiling

Total RNA isolated from the myometrial, non-del(7q) UL and del(7q) UL tissues from each of 11 cases was assessed for quality by RNA Nano LabChip analysis on an Agilent Bioanalyzer 2100. Standard protocols as described in the Affymetrix GeneChip Expression Analysis Technical Manual revision 4 (http://jaxservices.jax.org/Affymetrix_Gene_expression_manual_430.pdf) were employed at the Harvard Medical School - Partners HealthCare Center for Genetics and Genomics (HPCGG). Briefly, 5 μg total RNA template from each sample was reverse-transcribed into cDNA using oligo-dT primer containing T7 RNA polymerase binding sites using the GeneChip Expression 3'-Amplification Reagents One-Cycle cDNA Synthesis kit with subsequent purification of the double-stranded product with Affymetrix GeneChip Cleanup Module (Affymetrix, Santa Clara, CA). *In vitro* transcription to produce complementary RNA (cRNA) using T7 Polymerase and biotinylated dUTP and dCTP was performed with the GeneChip Expression Amplification Reagents kit (Affymetrix) and the biotin labeled

product quantitated on a Bio-Tek UV plate reader (Bio-Tek, Winooski, VT). Following purification and fragmentation to reduce secondary structure, hybridization in a Model 640 hybridization chamber to GeneChip Human Genome U133 Plus 2.0 oligonucleotide expression microarrays (Affymetrix), which contain over 54,000 oligonucleotide probe sets representing more than 47,000 transcripts and 38,500 well-characterized genes, occurred overnight at 45°C. Arrays were washed using a Model 450 Fluidics station with GeneChip Operating Software (Affymetrix). The GeneChip Model 3000 7G was employed to scan the arrays and the probe set expression values were calculated by GeneChip software using the MAS 5.0 algorithm. Array images were inspected visually for experimental artifacts and various quality measurements such as presence calls and RNA degradation were examined to verify the quality of the data.

Data processing and analysis were carried out in the statistical language R (R Development Core Team, 2008), including the use of microarray analysis tools from the Bioconductor project (Gentleman et al., 2004). Normalization across arrays occurred by setting the trimmed (2% of each tail) mean of each array to 100. Probe sets with fewer than five present calls among the del(7q) UL, non-del(7q) UL, and myometrium arrays were excluded. Paired differential expression analysis (not accounting for percent mosaicism) between del(7q) UL and non-del(7q) UL was computed using paired t-tests in which tissue samples were analyzed as matched pairs based on patient status. Mosaicism-weighted paired differential expression analysis was implemented in the Bioconductor package *limma* (Smyth, 2005) by fitting a linear model (Gentleman et al., 2004) with weights equal to the percent mosaicism for each array. All differential expression analyses were corrected for multiple testing using the false discovery rate (Q-value).

Expression data were deposited at the NCBI Gene Expression Omnibus (GEO; http://www.ncbi.nlm.nih.gov/geo/); the series entry number is GSE12814 and the specific accession identifiers are listed in Table 1.

Ingenuity Pathways Analysis

Functional analyses of the top 300 probe sets from the del(7q) UL-specific gene list weighted for del(7q) cell mosaicism were performed using Ingenuity Pathways Analysis (IPA, Ingenuity Systems, Redwood City, CA, USA, www.Ingenuity.com) through uploading of the Affymetrix probe set identifiers and fold changes. Networks were generated by looking for interactions of the del(7q) UL-specific genes to others based on the published literature accumulated in the Ingenuity Pathways Knowledge Base. Fisher's exact test was used to assign statistical significance, which is displayed as a score based on –log(P-value) and represents the probability of finding genes from the del(7q) UL-specific gene list in a network relative to genes being assembled into that network based on random chance. A score greater than two indicates less than a one in 100 likelihood (P –value < 0.01) that genes are assembled into a network by random chance. Networks including > 25 genes from the del(7q) UL-specific list are highly significant (giving a score of > 50).

RESULTS

Screening for del(7q) UL by Interphase FISH and Karyotyping

To identify UL with deletions in 7q22, interphase FISH or karyotype analysis was employed (Table 1). For del(7q) interphase FISH, a conservative false-positive cut-off of 9% monosomy was established by doubling the positive rate of 4.5% found in normal peripheral blood lymphocytes. Probe binding to the correct target region without cross-hybridization was validated on lymphocyte metaphases. The probe (RP11-374e17 at 7q22.2) was chosen based on its presence within the commonly deleted interval among five prior del(7q) UL

LOH studies (Ishwad et al., 1997;Sell et al., 1998;van der Heijden et al., 1998;Saito et al., 2005;Vanharanta et al., 2005). Screening of 206 tumors identified 19 UL with at least partial deletion of 7q22 (9.2%). Of these 19 UL, those with parallel myometrium and non-del(7q) samples plus similar cases found through karyotyping were selected for further analysis resulting in a total of 11 cases. The level of mosaicism in these 11 cases of cells with del(7q) ranged from 12–80%. Case 5 also had a proportion of cells with another recurrent UL karyotypic abnormality, t(12;14)(q15;q23-q24).

Identification of del(7q)-Specific UL Genes

RNA from each del(7q) UL as well as from concurrently collected non-del(7q) UL and normal myometrial tissues from each of 11 cases was hybridized on Affymetrix GeneChip Human Genome U133 Plus 2.0 oligonucleotide arrays for expression analysis. Among these cases, multiple clinical features were variable such as UL size, race, and the patient age and stage of menstrual cycle at the time of surgical removal (Table 2). To control for such variables, a direct comparison of the array expression data was made between tissues obtained from each individual to identify differences in expression specifically resulting from the deletion. A heatmap from an unsupervised hierarchical cluster analysis of the 500 most variable genes demonstrates a tendency of the myometrial tissues to cluster separately from the UL samples and the del(7q) UL and non-del(7q) UL to cluster by patient rather than by presence or absence of the deletion (Fig. 1A). The separation of the myometrial samples from the overlapping UL groups can be visualized in three dimensions through principal component analysis (Fig. 1B). These results suggest incorporation of the myometrial array data is suited to determining genes that differentiate any UL from the normal myometrium tissue rather than identifying the del(7q)-specific UL genes. Therefore, the myometrial samples were not included in further analyses.

The effect of controlling for patient to patient variability is further illustrated by a comparison of the percent of genes overlapping between gene lists generated by a paired and an unpaired analysis of the del(7q) UL and non-del(7q) UL expression data. Minimal overlap was found between the two analyses, particularly among the most significant genes (Fig. 1C). A comparison of the top 50 genes from each analysis showed only 20% in common, a percentage which did not increase above 40% when extended to include the top several hundred genes. Another demonstration of the need to take into account variability between patients is shown by examining the distribution of p-values from paired and unpaired t-tests for a two group comparison (Fig. 1D). In the paired case, the individual variation is accounted for by considering the difference between the samples of the same individual, resulting in a peak on the left side of the distribution indicating more genes with significant p-values were identified than expected from a random data set. In contrast, the unpaired analysis ignores the sample pairing and results in a nearly flat distribution, showing no clear evidence that genes appearing to have significant p-values from such a study analysis design would be true positives.

Based on these analyses, paired t-tests directly contrasting the del(7q) UL and the non-del(7q) UL from each individual were performed to determine del(7q) associated genes. This resulted in a list of genes ordered by their genome-wide significance levels corrected for multiple testing by the false discovery rate (Q-value) (Storey and Tibshirani, 2003). Of the 100 most significant del(7q) UL-specific genes, those with decreased expression are reported in Table 3 and those with increased expression in Table 4. A more extensive data set of 300 genes is provided as Supplementary Table S1. Importantly, the del(7q) UL-specific gene list is highly enriched for genes localized to 7q, most of which are in the proposed target region of 7q22 (Fig. 2). Further, all genes in 7q22 showed decreased expression. One of these genes, the vesicle transport mediator *SYPL1* in 7q22.2, appears on

the del(7q) UL-specific gene list at number 227 and is overlapped by the FISH probe employed to identify the del(7q) UL.

Identification of del(7q)-Specific UL Genes Weighted for Percent Mosaicism of del(7q) Cells

Cells with 7q abnormalities in UL are usually present in a mosaic form with karyotypically normal cells (Xing et al., 1997). In contrast to previous studies, the impact of this biology was integrated by weighting each sample pair [del(7q) UL and non-del(7q) UL from the same woman] for percent del(7q) mosaicism of the tumor in a paired differential expression analysis: the higher the percentage of del(7q) cells present, the more heavily weighted was that sample. The 50 most significant genes based on Q-value in this modified del(7q) UL-specific gene list are given in Table 5. A more expansive list of 300 genes is also presented (Supplementary Table S2). The purpose of weighting the samples for mosaicism level is to compensate for background noise caused by the karyotypically normal cells in order to identify those genes specific to the del(7q) abnormality. The validity of this approach is supported by the two-fold increase in the proportion of genes in 7q22 within the top 50 of the mosaicism-weighted list relative to the non-weighted list (from 10 up to 20 genes). A comparison of the expression log ratios of genes and percent mosaicism identified seven genes with a Q-value ≤ 0.1 which are illustrated as scatterplots (Fig. 3A). Three of these seven significant genes are located in 7q22 (Fig. 3B).

Determination of Deletion Size Using aCGH and Alignment to Gene Expression Data

Genomic copy number changes in the del(7q) UL of six cases for which DNA was available was assessed using array comparative genomic hybridization (aCGH). The matched myometrium from each woman was used as the control against which each del(7q) UL DNA was compared to remove any copy number variants inherent in the patient but not related to tumorigenesis. All samples tested showed genomic deletion of 7q (Fig. 4A). The smallest commonly deleted region on chromosome 7 in all six samples spanned approximately 9.5 megabases from 7q22.1-q31.1 (Fig. 4B). No other deletion or amplification was universal to all samples (Supplementary Table S3). Alignment of this aCGH-defined commonly deleted region on 7q to the significant genes ($P < 0.01$) from the percent mosaicism-weighted del(7q) UL-specific list demonstrated a high correlation between genes located in the deletion interval and significantly downregulated expression (Fig. 4A). This correlation supports the accuracy of both the aCGH and expression microarray data. The significant genes in the commonly deleted interval are listed in Table 6.

Quantitative PCR (Q-PCR) Confirmation of MLL5 Expression

Cases 4, 7, 10 and 11 for which additional RNA was available were evaluated by Q-PCR for expression of *MLL5* (Mixed-Lineage Leukemia-5), a gene in 7q22.3 which had decreased expression in del(7q) UL by microarray analysis (sixth gene in the del(7q)-specific gene list). In addition, *MLL5* was significant with a Q-value of 0.0753 and a P-value of 0.0000148 in the fourth position in the gene list produced by weighting for percent mosaicism of del(7q) cells (Table 5). Q-PCR for *MLL5* confirmed the microarray data of a 1.4-fold reduction by showing a 1.5-fold decrease in RNA expression in the del(7q) UL compared to non-del(7q) UL after normalization to *GAPDH* (data not shown).

Functional Significance of del(7q)-Specific UL Genes

To extract biological insight from the transcriptional profile of del(7q) UL, the top 300 probe sets from the del(7q) mosaicism-weighted gene list, which represent the majority of genes with altered expression in the target region of 7q22, were investigated with the Ingenuity Pathways Analysis (IPA) System. IPA is a web-based entry tool developed by

systematic encoding of manually curated functional relationships between genes presented in hundreds of thousands of scientific publications. Of the 300 probe sets, 197 were assigned to networks. There were 19 networks of functional dependencies generated of which two were highly significant (score > 50, genes from deletion 7q list > 25); nodes in the network correspond to a gene and each arc to a published article reporting a functional relationship between those two linked genes. The most significant networks (Fig. 5A and 5B) are principally associated with development. The other networks involving 11 to 18 del(7q) UL-specific genes (scores 15 to 28) are associated with multiple functions including but not limited to cell cycle, cell growth, cancer, cell morphology, DNA replication and repair, reproductive system disease, gene expression, and additional development pathways.

In addition to functional networks, IPA was also used to identify which well-characterized canonical pathways are most relevant across the entire del(7q) UL dataset. The significance is based on a p-value calculated using the right-tailed Fisher's Exact Test by comparing the number of user-supplied genes that participate in a given function or pathway relative to the total number of occurrences of these genes in all function/pathway annotations stored in the Ingenuity pathways knowledge base. The protein ubiquitination pathway was the most significantly associated (P-value = 2.76×10^{-5}), involving 11 genes from the del(7q) UL-specific list. The genes from network 1 involved in protein ubiquitination include *PSMA2*, *PSMB3*, *PSMC2*, *PSMC3* while those in network 2 include *UBE2I* and *UBE2J1*.

DISCUSSION

Multiple recurrent cytogenetic abnormalities have been described in UL, suggesting these tumors develop from several distinct genetic pathways. This necessitates examination of each major cytogenetic subgroup for its role in UL tumorigenesis. One of the most common abnormalities, deletion or rearrangement of 7q22, remains largely undefined as determination of the causative gene(s) has been complicated by the uncertainty of the smallest commonly deleted region and the gene-dense nature of the target region 7q22.

Rearrangements of 7q22 are found more consistently in UL but have been observed in other solid tumors such as lipomas and endometrial polyps as well as some hematological malignancies (Dal Cin et al., 1995; Dal Cin et al., 1997; Liang et al., 1998). Such frequent deletion or rearrangement of a specific chromosomal region is generally thought to indicate involvement of a tumor suppressor gene where tumorigenesis results from the structural loss of one copy and subsequent mutation of the other allele. However, it remains unclear if UL with chromosome 7 abnormalities follow a loss of function pattern either due to deletion or disruption at the translocation breakpoint. Alternatively, haploinsufficiency may be the underlying molecular mechanism. Another possibility is that del(7q) UL arise through a gain of function, resulting from either production of a fusion gene or a positional effect due to rearranging sequences within chromosome 7 such as by an interstitial deletion. A gain of function is not as likely because the del(7q) breakpoints are variable. It also has yet to be determined if the predisposing gene(s) at 7q22 is the same or divergent between UL, other mesenchymal solid tumors, and myeloid cells (AML and MDS).

Multiple studies have targeted del(7q) UL and shown LOH of microsatellite markers or altered expression of genes within 7q22 such as *CUTL1* (repressor of *c-MYC* expression), *ORC5L* (DNA replication initiation factor), *LAMB1* (extracellular matrix component), *LHFPL3* (transmembrane protein of unknown function), and *PAI1* (hemostasis and smooth muscle cell expression) (Sourla et al., 1996; Zeng et al., 1997; Quintana et al., 1998; Saito et al., 2005; Ptacek et al., 2007). No alteration in expression was found by RT-PCR for *NRCAM*, *DLD*, *PIK3G*, *PBEF* or *SRPK2* (Saito et al., 2005). However, despite these varied

efforts, no consistent gene expression changes have been identified and the causative gene(s) in the pathogenesis of the del(7q) subgroup of UL remain to be established.

It is notable that UL with 7q abnormalities are often mosaic with karyotypically normal 46,XX cells and when cultured grow poorly and frequently lose the chromosomally aberrant cell line (Xing et al., 1997). These observations indicate a gene(s) deleted from the 7q region likely plays a role in regulating cellular growth (Rein et al., 1998). Such mosaic UL were demonstrated to be clonal tumors, which may suggest the del(7q) abnormality is not likely to be the primary pathogenetic event. Deletion of 7q has however been observed as the sole abnormality in a non-mosaic state, and it is possible there are submicroscopic pathogenetic events such as small deletions or point mutations in the regulatory or coding sequences occurring in the same genes as those indicated by chromosomal rearrangement (Xing et al., 1997). In fact, submicroscopic deletions have been identified by the finding of LOH in 7q in a subset of karyotypically normal UL through microsatellite allelotyping (Ishwad et al., 1997).

Further inconsistency has been noticed when attempting to correlate LOH and karyotype data. LOH was not detected in a proportion of UL with cytogenetically visible 7q deletions (Ishwad et al., 1997). This discrepant result may be due to the mosaic nature of these UL where the karyotypically normal cells dilute the ability of aCGH to detect the change in DNA copy number of the involved genes. Another explanation is that del(7q) tumors identified solely by interphase FISH may have rare complex chromosomal rearrangements which result in some 7q genes being integrated elsewhere in the genome.

In addition to an inability to detect complex rearrangements, FISH is not able to quantify precisely the deletion interval size. Defining the deletion boundaries was therefore addressed in the current study by employing aCGH analysis on six of the del(7q) UL. In contrast to earlier work that employed aCGH using a general female normal DNA as the control (Vanharanta et al., 2007), we used the normal myometrial tissue from the same patient as the control in each case to eliminate any confounding effect of germline copy number variation. The only consistent copy number change among the six cases analyzed was deletion on chromosome 7, the smallest common region of which spanned approximately 9.5 megabases from 7q22.1-q31.1. Alignment of genes significantly expressed in del(7q) UL relative to non-del(7q) UL after correction for mosaicism demonstrated a high correlation between gene presence in the common deletion interval and decreased expression. This provides a further validation of the accuracy of the microarray expression data. Our results also confirm the finding that small homozygous deletions are not observed in del(7q) UL, arguing against the target gene(s) in 7q being a tumor suppressor. In fact, microarray expression analysis and coding region sequencing of many genes across the region have previously failed to identify a gene of interest (Vanharanta et al., 2005; Vanharanta et al., 2007).

Other microarray expression analyses of UL relied on a comparison of the tumors to the normal myometrial tissue, not taking into account the known cytogenetic variation among UL. To identify genes specific to the del(7q) abnormality rather than those that distinguish myometrium from any UL, the expression profile of del(7q) UL needs to be compared directly to that of non-del(7q) UL. The current study takes this approach, and in contrast to recent work (Vanharanta et al., 2005), the del(7q) and non-del(7q) tumors were from the same rather than different patients to eliminate the genotype, environment, and genotype x environment confounding effects that underlie patient to patient variation. In addition, the aforementioned study employed the HG-U133A array which has less extensive genome coverage than the U133 plus 2.0 microarray used in the present work, and even after reducing the stringency to identify any contrasting genes of significance, none were discovered in their 7q commonly deleted region (Vanharanta et al., 2005).

The validity and necessity of our approach to compare UL with and without the abnormality from the same patient is supported by the finding of a del(7q) UL-specific gene list that is highly enriched for genes in 7q22, all of which showed significantly decreased expression. It is interesting that the chromatin-modulating gene *MLL5* (Mixed Lineage Leukemia-5), which is ranked sixth in the del(7q) UL-specific gene list and was examined by Q-PCR to confirm the decreased expression observed by microarray data analysis, has been found to inhibit cancer cell cycle progression when ectopically overexpressed or when knocked down by small interfering RNAs (Deng et al., 2004; Cheng et al., 2008). This suggests cells are very sensitive to *MLL5* dosage, and haploinsufficiency due to deletion at 7q22.3 in UL may explain at least in part the poor growth and frequent loss of the abnormal cell line in culture as well as a relatively smaller size of del(7q) tumors compared to another UL subgroup, those with a t(12;14)(q15;q23-q24) (Rein et al., 1998).

MLL5 was found to reach statistical significance and rank fourth on the del(7q) UL-specific gene list when the data were weighted for the percent of cells containing the 7q deletion. Previous studies had not accounted for the mosaic nature of most del(7q) UL, and the doubling of genes at 7q22 in the top 50 of the mosaicism-weighted gene list relative to the unweighted list (from 10 up to 20 genes) suggests the importance of implementing this data correction to reduce the noise introduced by karyotypically normal cells. Six other genes (*ZNF498*, *TRAF3IP1*, *MGC39821*, *SSR2*, *MARCKS*, and *HBP1*) were also identified as being significant. *HBP1* at 7q22.3 is of interest as loss of expression of this proliferation repressor has been associated with invasive breast cancer, suggesting the decreased expression found in del(7q) UL may contribute to the proliferative capacity of these tumors (Paulson et al., 2007). A similarly functioning gene, *SIN3A* at 15q24.2, also has decreased expression in del(7q) UL and is present at number 155 on the mosaicism weighted gene list (also in network 2 as described below). *SIN3A* is a core component of a complex with histone deacetylase enzyme activity which is employed by multiple factors such as p53 to repress their target genes such that loss of *SIN3A* activity is linked to proliferation and cell survival (Dannenberg et al., 2005). Downregulation of *SIN3A* has been demonstrated in human cancer, specifically non-small cell lung type (Suzuki et al., 2008). Another gene of significance in the del(7q) UL mosaicism-weighted list is *RINT1*, which has been shown through RNA interference studies and the development of multiple tumors in haploinsufficient mice to serve a novel tumor suppressor function by maintaining integrity of the Golgi apparatus and centrosome necessary for proper cell division (Lin et al., 2007).

Biological insight into del(7q) UL was pursued further through Ingenuity Pathways Analysis (IPA) of the top 300 probe sets based on the Q-value from the del(7q) mosaicism-weighted gene list. The two networks of highest significance were associated with development, which may reflect the need of the tumor cells to revert towards a more embryonic phenotype to proliferate. This could be related to the hypothesis that UL arise from an inappropriate activation of myometrial cell proliferation deriving from the inherent abilities of the uterine tissue during pregnancy (Andersen et al., 1995). Interestingly, the most represented canonical pathway was protein ubiquitination, with 11 of the top 300 del(7q) UL-specific genes. Genes from network 1 involved in protein ubiquitination include *PSMA2*, *PSMB3*, *PSMC2*, and *PSMC3* while those in network 2 include *UBE2I* and *UBE2J1*. Ubiquitination is of interest because >80% of cellular proteins are tagged with ubiquitin for proteasome degradation and cancer can develop through disruption of this system either by stabilizing oncoproteins or destabilizing tumor suppressor genes (Burger and Seth, 2004). The hierarchical nature of the ubiquitination enzyme cascade with transfer from E1 to any of a multitude of E2s and then E3s as well as a number of different subunits present on the proteasome allows for specialization targeting of proteins for degradation. It is therefore likely that disruption of multiple E2 enzymes (EBE2 genes) and proteasome subunits (PSM

genes) reflects an altered protein homeostasis in the del(7q) UL which potentially contributes to tumorigenesis.

In conclusion, this study provides a genome-wide expression profile of the 7q deletion cytogenetic subgroup of UL. The unique design employed to target del(7q) UL-specific genes included a paired comparison to non-del(7q) UL from the same women and weighting of the data for percent of del(7q) cells to account for the mosaicism usually present in this UL subgroup. Although the full implications and biological significance of the differentially expressed genes and networks remain to be fully elucidated, the resultant gene list, which is dense with genes from the target region of 7q22, may serve as a platform to explore further relevant mechanisms of tumor pathogenesis and understanding of the molecular basis of UL.

Supplementary Material

Refer to Web version on PubMed Central for supplementary material.

Acknowledgments

The authors would like to thank David Zahrieh at Dana-Farber Cancer Institute for helpful discussions and exploration of the data by ANOVA and Karen T.Cuenco at the University of Pittsburgh for a thoughtful review of the manuscript.

Supported by: This work was supported by NIH grants RO1HD046226 and RO1CA78895 (to CCM) and JCH was supported by T32GM007748.

REFERENCES

Andersen J, DyReyes VM, Barbieri RL, Coachman DM, Miksicek RJ. Leiomyoma primary cultures have elevated transcriptional response to estrogen compared with autologous myometrial cultures. J Soc Gynecol Investig. 1995; 2:542–551.

Burger AM, Seth AK. The ubiquitin-mediated protein degradation pathway in cancer: therapeutic implications. Eur J Cancer. 2004; 40:2217–2229. [PubMed: 15454246]

Buttram VC Jr, Reiter RC. Uterine leiomyomata: etiology, symptomatology, and management. Fertil Steril. 1981; 36:433–445. [PubMed: 7026295]

Cheng F, Liu J, Zhou SH, Wang XN, Chew JF, Deng LW. RNA interference against mixed lineage leukemia 5 resulted in cell cycle arrest. Int J Biochem Cell Biol. 2008; 40:2472–2481. [PubMed: 18573682]

Cheung VG, Nowak N, Jang W, Kirsch IR, Zhao S, Chen XN, Furey TS, Kim UJ, Kuo WL, Olivier M, Conroy J, Kasprzyk A, Massa H, Yonescu R, Sait S, Thoreen C, Snijders A, Lemyre E, Bailey JA, Bruzel A, Burrill WD, Clegg SM, Collins S, Dhami P, Friedman C, Han CS, Herrick S, Lee J, Ligon AH, Lowry S, Morley M, Narasimhan S, Osoegawa K, Peng Z, Plajzer-Frick I, Quade BJ, Scott D, Sirotkin K, Thorpe AA, Gray JW, Hudson J, Pinkel D, Ried T, Rowen L, Shen-Ong GL, Strausberg RL, Birney E, Callen DF, Cheng JF, Cox DR, Doggett NA, Carter NP, Eichler EE, Haussler D, Korenberg JR, Morton CC, Albertson D, Schuler G, de Jong PJ, Trask BJ. Integration of cytogenetic landmarks into the draft sequence of the human genome. Nature. 2001; 409:953–958. [PubMed: 11237021]

Coronado GD, Marshall LM, Schwartz SM. Complications in pregnancy, labor, and delivery with uterine leiomyomas: a population-based study. Obstet Gynecol. 2000; 95:764–769. [PubMed: 10775744]

Cramer SF, Patel A. The frequency of uterine leiomyomas. Am J Clin Pathol. 1990; 94:435–438. [PubMed: 2220671]

Dal Cin P, Van den Berghe H, Sciot R, de Wever I. Deletion of the long arm of chromosome 7 in lipoma. Cancer Genet Cytogenet. 1997; 96:85–86. [PubMed: 9209475]

Dal Cin P, Vanni R, Marras S, Moerman P, Kools P, Andria M, Valdes E, Deprest J, Van de Ven W, Van den Berghe H. Four cytogenetic subgroups can be identified in endometrial polyps. Cancer Res. 1995; 55:1565–1568. [PubMed: 7882366]

Dannenberg JH, David G, Zhong S, van der Torre J, Wong WH, Depinho RA. mSin3A corepressor regulates diverse transcriptional networks governing normal and neoplastic growth and survival. Genes Develop. 2005; 19:1581–1595. [PubMed: 15998811]

Deng LW, Chiu I, Strominger JL. MLL 5 protein forms intranuclear foci, and overexpression inhibits cell cycle progression. Proc Natl Acad Sci U S A. 2004; 101:757–762. [PubMed: 14718661]

Flynn M, Jamison M, Datta S, Myers E. Health care resource use for uterine fibroid tumors in the United States. Am J Obstet Gynecol. 2006; 195:955–964. [PubMed: 16723104]

Gentleman RC, Carey VJ, Bates DM, Bolstad B, Dettling M, Dudoit S, Ellis B, Gautier L, Ge Y, Gentry J, Hornik K, Hothorn T, Huber W, Iacus S, Irizarry R, Leisch F, Li C, Maechler M, Rossini AJ, Sawitzki G, Smith C, Smyth G, Tierney L, Yang JY, Zhang J. Bioconductor: open software development for computational biology and bioinformatics. Genome Biol. 2004; 5:R80. [PubMed: 15461798]

Hartmann KE, Birnbaum H, Ben-Hamadi R, Wu EQ, Farrell MH, Spalding J, Stang P. Annual costs associated with diagnosis of uterine leiomyomata. Obstet Gynecol. 2006; 108:930–937. [PubMed: 17012456]

Hashimoto K, Azuma C, Kamiura S, Kimura T, Nobunaga T, Kanai T, Sawada M, Noguchi S, Saji F. Clonal determination of uterine leiomyomas by analyzing differential inactivation of the X-chromosome-linked phosphoglycerokinase gene. Gynecol Obstet Invest. 1995; 40:204–208. [PubMed: 8529956]

Ishwad CS, Ferrell RE, Hanley K, Davare J, Meloni AM, Sandberg AA, Surti U. Two discrete regions of deletion at 7q in uterine leiomyomas. Genes Chromosomes Cancer. 1997; 19:156–160. [PubMed: 9218996]

Karolchik D, Baertsch R, Diekhans M, Furey TS, Hinrichs A, Lu YT, Roskin KM, Schwartz M, Sugnet CW, Thomas DJ, Weber RJ, Haussler D, Kent WJ. The UCSC Genome Browser Database. Nucleic Acids Res. 2003; 31:51–54. [PubMed: 12519945]

Lepine LA, Hillis SD, Marchbanks PA, Koonin LM, Morrow B, Kieke BA, Wilcox LS. Hysterectomy surveillance--United States, 1980–1993. MMWR CDC Surveill Summ. 1997; 46:1–15. [PubMed: 9259214]

Liang H, Fairman J, Claxton DF, Nowell PC, Green ED, Nagarajan L. Molecular anatomy of chromosome 7q deletions in myeloid neoplasms: evidence for multiple critical loci. Proc Natl Acad Sci U S A. 1998; 95:3781–3785. [PubMed: 9520444]

Lin X, Liu CC, Gao Q, Zhang X, Wu G, Lee WH. RINT-1 serves as a tumor suppressor and maintains Golgi dynamics and centrosome integrity for cell survival. Mol Cell Biol. 2007; 27:4905–4916. [PubMed: 17470549]

Mashal RD, Fejzo ML, Friedman AJ, Mitchner N, Nowak RA, Rein MS, Morton CC, Sklar J. Analysis of androgen receptor DNA reveals the independent clonal origins of uterine leiomyomata and the secondary nature of cytogenetic aberrations in the development of leiomyomata. Genes Chromosomes Cancer. 1994; 11:1–6. [PubMed: 7529041]

Meloni AM, Surti U, Contento AM, Davare J, Sandberg AA. Uterine leiomyomas: cytogenetic and histologic profile. Obstet Gynecol. 1992; 80:209–217. [PubMed: 1635734]

Moore SD, Herrick SR, Ince TA, Kleinman MS, Cin PD, Morton CC, Quade BJ. Uterine leiomyomata with t(10;17) disrupt the histone acetyltransferase MORF. Cancer Res. 2004; 64:5570–5577. [PubMed: 15313893]

Nibert M, Heim S. Uterine leiomyoma cytogenetics. Genes Chromosomes Cancer. 1990; 2:3–13. [PubMed: 2278965]

Ozisik YY, Meloni AM, Surti U, Sandberg AA. Deletion 7q22 in uterine leiomyoma. A cytogenetic review. Cancer Genet Cytogenet. 1993; 71:1–6. [PubMed: 8275445]

Paulson KE, Rieger-Christ K, McDevitt MA, Kuperwasser C, Kim J, Unanue VE, Zhang X, Hu M, Ruthazer R, Berasi SP, Huang CY, Giri D, Kaufman S, Dugan JM, Blum J, Netto G, Wazer DE, Summerhayes IC, Yee AS. Alterations of the HBP1 transcriptional repressor are associated with invasive breast cancer. Cancer Res. 2007; 67:6136–6145. [PubMed: 17616670]

Ptacek T, Song C, Walker CL, Sell SM. Physical mapping of distinct 7q22 deletions in uterine leiomyoma and analysis of a recently annotated 7q22 candidate gene. Cancer Genet Cytogenet. 2007; 174:116–120. [PubMed: 17452252]

Quintana DG, Thome KC, Hou ZH, Ligon AH, Morton CC, Dutta A. ORC5L, a new member of the human origin recognition complex, is deleted in uterine leiomyomas and malignant myeloid diseases. J Biol Chem. 1998; 273:27137–27145. [PubMed: 9765232]

Rein MS, Friedman AJ, Barbieri RL, Pavelka K, Fletcher JA, Morton CC. Cytogenetic abnormalities in uterine leiomyomata. Obstet Gynecol. 1991; 77:923–926. [PubMed: 2030869]

Rein MS, Nowak RA. Biology of uterine myomas and myometrium in vitro. Sem Repro Endocrin. 1992; 10:310–319.

Rein MS, Powell WL, Walters FC, Weremowicz S, Cantor RM, Barbieri RL, Morton CC. Cytogenetic abnormalities in uterine myomas are associated with myoma size. Mol Hum Reprod. 1998; 4:83–86. [PubMed: 9510016]

Saito E, Okamoto A, Saito M, Shinozaki H, Takakura S, Yanaihara N, Ochiai K, Tanaka T. Genes associated with the genesis of leiomyoma of the uterus in a commonly deleted chromosomal region at 7q22. Oncol Rep. 2005; 13:469–472. [PubMed: 15706419]

Sargent MS, Weremowicz S, Rein MS, Morton CC. Translocations in 7q22 define a critical region in uterine leiomyomata. Cancer Genet Cytogenet. 1994; 77:65–68. [PubMed: 7923086]

Sell SM, Altungoz O, Prowse AA, Meloni AM, Surti U, Sandberg AA. Molecular analysis of chromosome 7q21.3 in uterine leiomyoma: analysis using markers with linkage to insulin resistance. Cancer Genet Cytogenet. 1998; 100:165–168. [PubMed: 9428363]

Sell SM, Tullis C, Stracner D, Song CY, Gewin J. Minimal interval defined on 7q in uterine leiomyoma. Cancer Genet Cytogenet. 2005; 157:67–69. [PubMed: 15676150]

Smyth, G., editor. Limma: linear models for microarray data. New York: Springer; 2005. p. 397-420.

Sourla A, Polychronakos C, Zeng WR, Nepveu A, Kukuvitis A, Naud F, Koutsilieris M. Plasminogen activator inhibitor 1 messenger RNA expression and molecular evidence for del(7)(q22) in uterine leiomyomas. Cancer Res. 1996; 56:3123–3128. [PubMed: 8674071]

Storey JD, Tibshirani R. Statistical significance for genomewide studies. Proc Natl Acad Sci U S A. 2003; 100:9440–9445. [PubMed: 12883005]

Suzuki H, Ouchida M, Yamamoto H, Yano M, Toyooka S, Aoe M, Shimizu N, Date H, Shimizu K. Decreased expression of the SIN3A gene, a candidate tumor suppressor located at the prevalent allelic loss region 15q23 in non-small cell lung cancer. Lung Cancer. 2008; 59:24–31. [PubMed: 17854949]

van der Heijden O, Chiu HC, Park TC, Takahashi H, LiVolsi VA, Risinger JI, Barrett JC, Berchuck A, Evans AC, Behbakht K, Menzin AW, Liu PC, Benjamin I, Morgan MA, King SA, Rubin SC, Boyd J. Allelotype analysis of uterine leiomyoma: localization of a potential tumor suppressor gene to a 4-cM region of chromosome 7q. Mol Carcinogenesis. 1998; 23:243–247.

Vanharanta S, Wortham NC, Laiho P, Sjoberg J, Aittomaki K, Arola J, Tomlinson IP, Karhu A, Arango D, Aaltonen LA. 7q deletion mapping and expression profiling in uterine fibroids. Oncogene. 2005; 24:6545–6554. [PubMed: 15940248]

Vanharanta S, Wortham NC, Langford C, El-Bahrawy M, van der Spuy Z, Sjoberg J, Lehtonen R, Karhu A, Tomlinson IP, Aaltonen LA. Definition of a minimal region of deletion of chromosome 7 in uterine leiomyomas by tiling-path microarray CGH and mutation analysis of known genes in this region. Genes Chromosomes Cancer. 2007; 46:451–458. [PubMed: 17285575]

Xing YP, Powell WL, Morton CC. The del(7q) subgroup in uterine leiomyomata: genetic and biologic characteristics. Further evidence for the secondary nature of cytogenetic abnormalities in the pathobiology of uterine leiomyomata. Cancer Genet Cytogenet. 1997; 98:69–74.

Zeng WR, Scherer SW, Koutsilieris M, Huizenga JJ, Filteau F, Tsui LC, Nepveu A. Loss of heterozygosity and reduced expression of the CUTL1 gene in uterine leiomyomas. Oncogene. 1997; 14:2355–2365. [PubMed: 9178912]

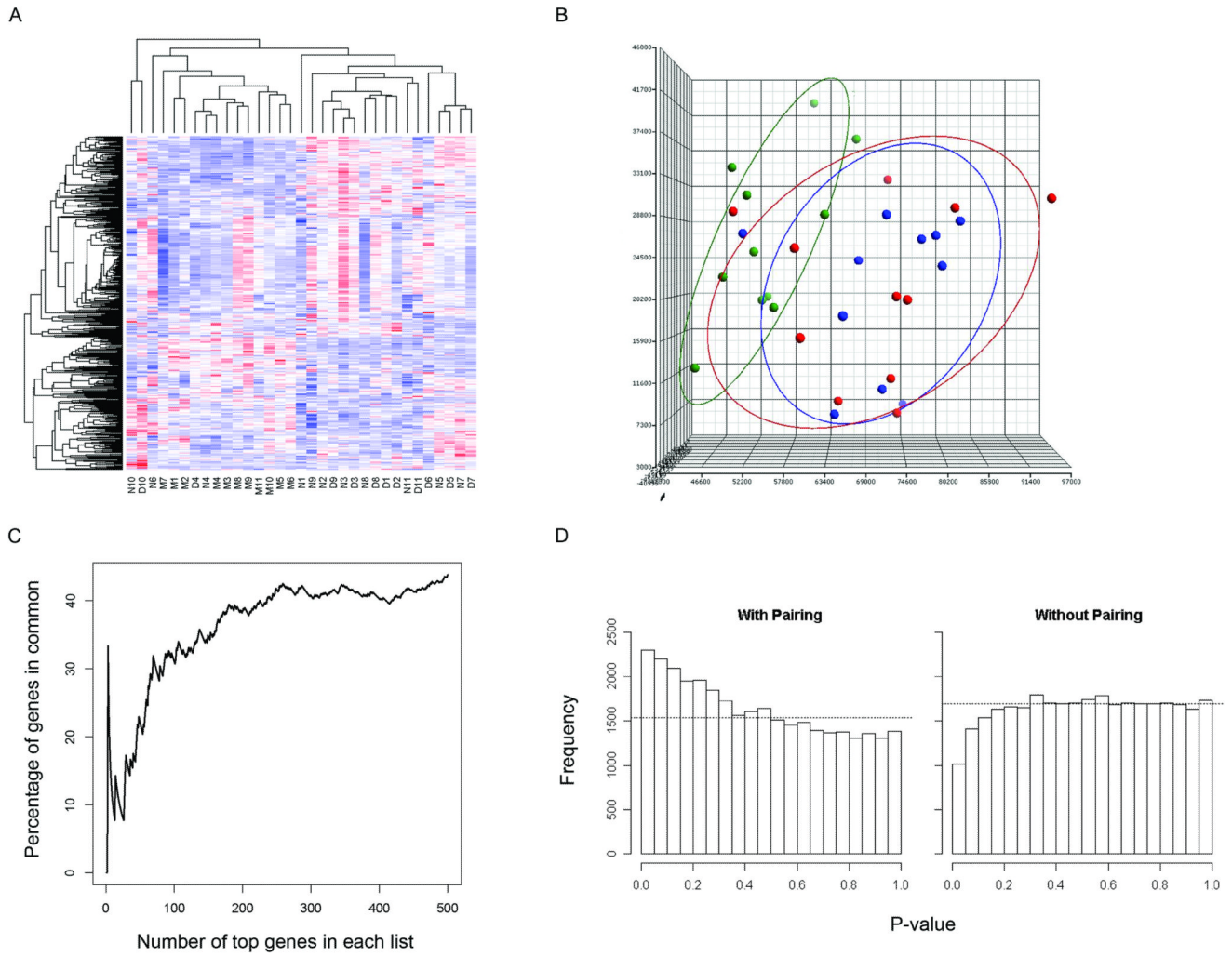

Figure 1.

Paired analysis of the del(7q) UL and non-del(7q) UL microarray data to control for patient to patient variability without involvement of the myometrium is necessary to generate an accurate del(7q) UL-specific gene list. (A) Heatmap of an unsupervised hierarchical cluster analysis of the 500 most variable genes between myometrium (M), del(7q) UL (D) and non-del(7q) UL (N) from each of the 11 patients shows a trend of myometrial separation from all UL tissues and of UL clustering based on patient rather than del(7q) status. A similar result is obtained when more genes are included in the analysis. (B) Unsupervised principal component analysis illustrates in three dimensions the tendency of the myometrial samples (Liang et al.) to cluster and have only minimal overlap with the del(7q) (blue) and non-del(7q) tissues (red). (C) A comparison of the percent of genes in common between a paired and unpaired analysis of del(7q) UL versus non-del(7q) UL indicates the two modes of analysis produce different gene lists. (D) The distribution of p-values for two group comparison t-tests using a paired analysis (with pairing) includes a peak on the left side indicating more genes were found with significant p-values than expected in a random data set. In contrast, the unpaired analysis (without pairing) generates a nearly flat distribution suggesting the genes with significant p-values identified by such an assessment are not likely to be true positives.

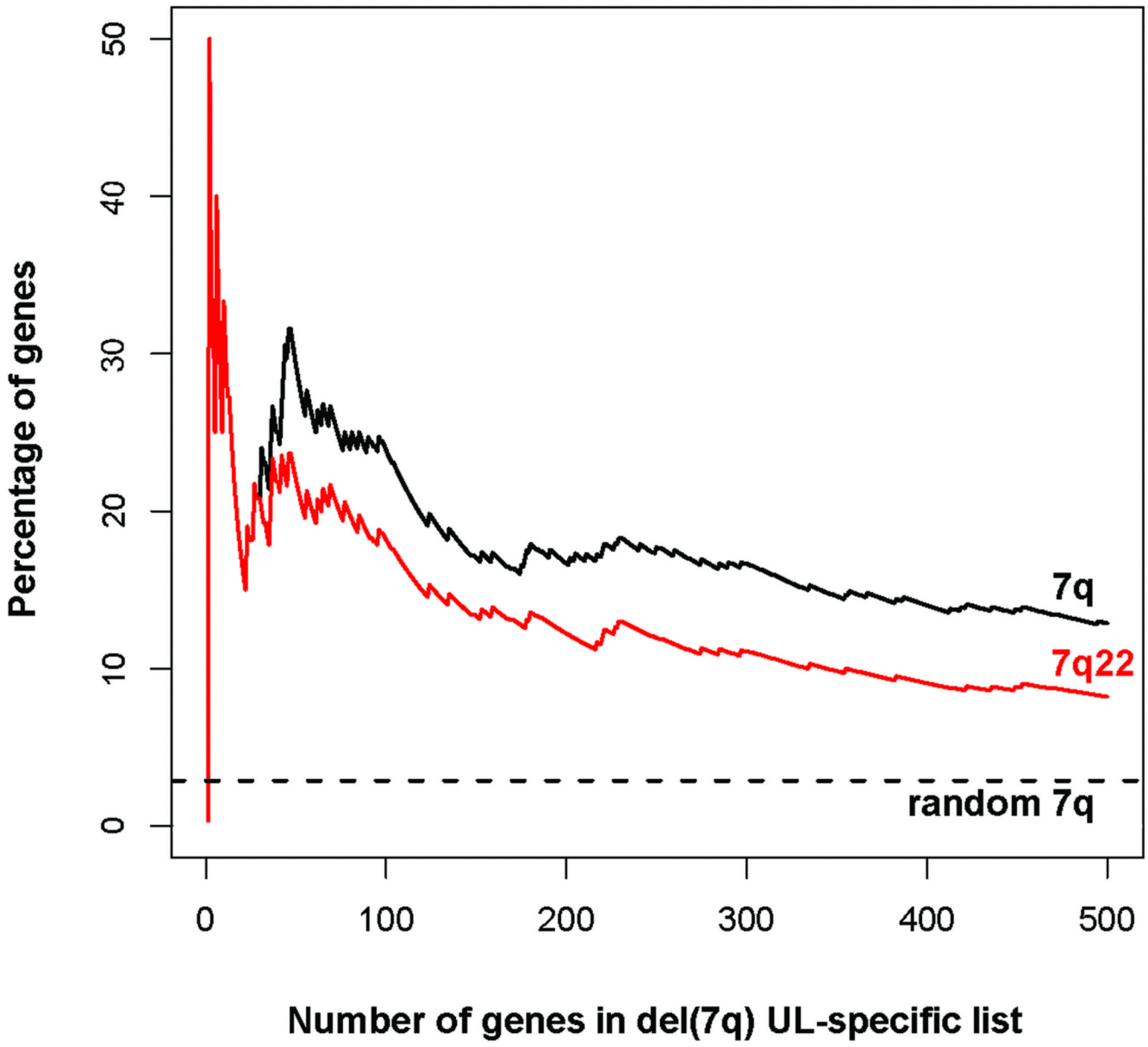

Figure 2.

The del(7q) UL-specific gene list is highly enriched for 7q genes. Examination of the top 500 genes based on false discovery rate shows a high percentage were localized to 7q (black line), the majority of which are in the proposed target region of 7q22 (red line). The more limited the gene list examined, the greater the percentage of genes mapped in 7q. This is in contrast to the expected percentage of genes in 7q if the list was generated randomly based on the fraction of genes in 7q in the total data (dotted line).

A

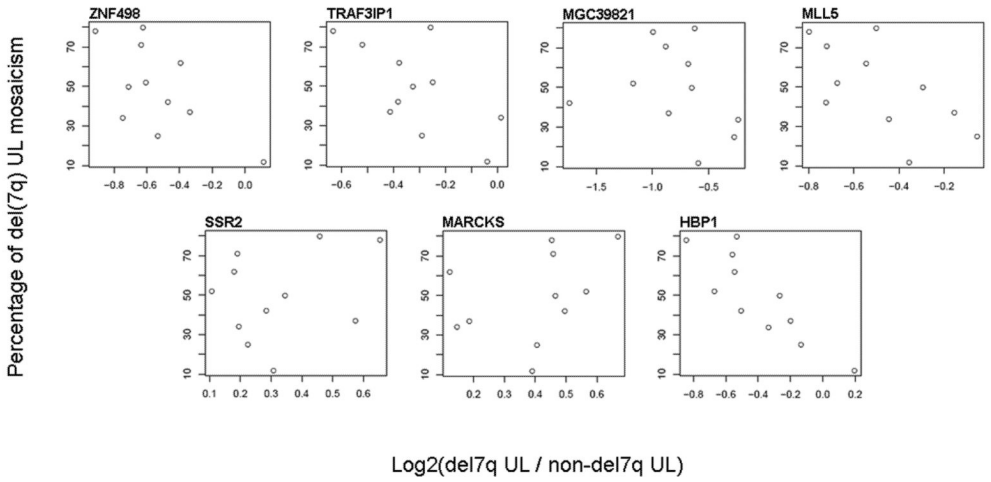

B

Gene Symbol	Gene Name	Probe Set	Ref Seq	Fold Change	P-value	Q-value	Chromosome
ZNF498	zinc finger protein 498	228138_at	NM_145115	-1.42	9.56E-07	0.0239	7q22.1
TRAF3IP1	TNF receptor-associated factor 3 interacting protein 1	238494_at	NM_015650	-1.23	9.49E-06	0.0753	2q37.3
MGC39821	hypothetical protein MGC39821	1555363_s_at	XR_041448	-1.67	1.23E-05	0.0753	19p13.11
MLL5	myeloid/lymphoid or mixed-lineage leukemia 5	226100_at	NM_018682	-1.37	1.48E-05	0.0753	7q22.1
SSR2	signal sequence receptor, beta	200652_at	NM_003145	1.26	1.52E-05	0.0753	1q21-q23
MARCKS	myristoylated alanine-rich protein kinase C substrate	225897_at	NM_002356	1.32	1.81E-05	0.0753	6q22.2
HBP1	HMG-box transcription factor 1	209102_s_at	NM_012257	-1.29	2.96E-05	0.1060	7q22-q31

Figure 3.

Seven most significant genes identified by weighting the microarray data for the level of del(7q) cell mosaicism in each UL. (A) Scatter plots show the relationship between the percent of del(7q) cells in each UL and the log ratio of gene expression in del(7q) UL relative to the non-del(7q) UL in each of the 11 women. (B) The significance of these seven genes is reflected by a Q-value ≤ 0.10, and three of the genes are in the region of interest at 7q22.

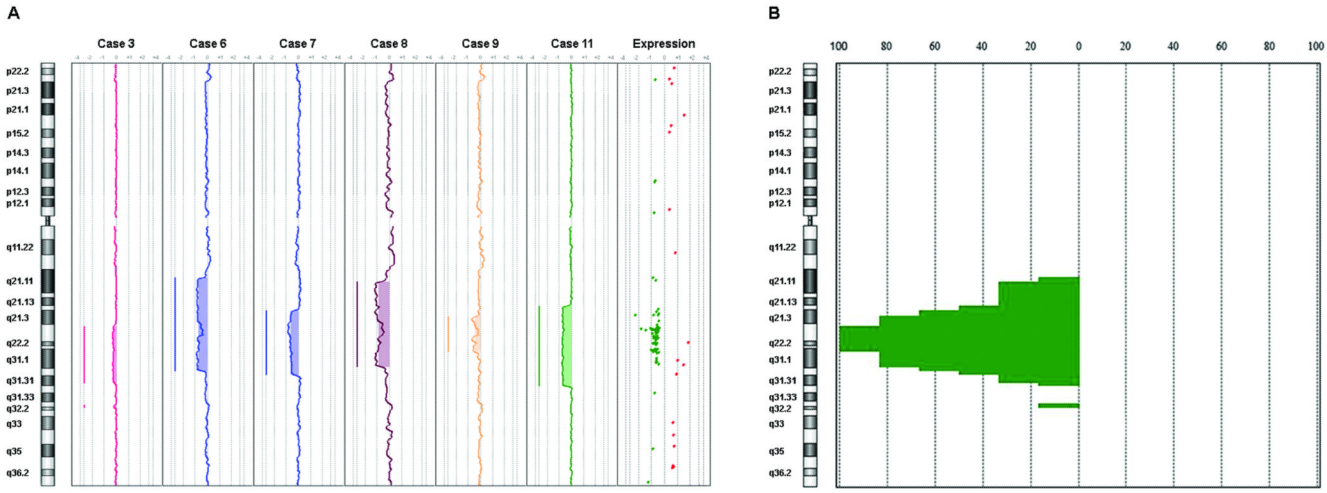

Figure 4.

Detection of a commonly deleted region using aCGH analysis of six del(7q) UL cases and alignment with microarray expression data showed a strong correlation between the 7q deletion and decreased gene expression. (A) aCGH analysis demonstrated variable 7q deletion sizes in each of the six cases. Alignment of the common deletion interval to genes with significant expression from the mosaicism-weighted del(7q) UL-specific gene list revealed a cluster of downregulated genes in the deleted interval, supporting the accuracy of the microarray expression analysis. Green dots represent downregulated genes and red dots upregulated genes. (B) Genomic penetrance summary of chromosome 7 showing the affected regions and in what percentage of the six cases they were found to be abnormal. Skewing of data to the left of zero indicates deletion. The common region of genomic loss for the six cases, as indicated by the 100% line, spans approximately 9.5 megabases from 7q22.1-q31.1 (basepairs 98,598,014–108,112,352 based on the UCSC genome browser March 2006 assembly; aCGH probe A_16_P18041391 to A_16_P18063689).

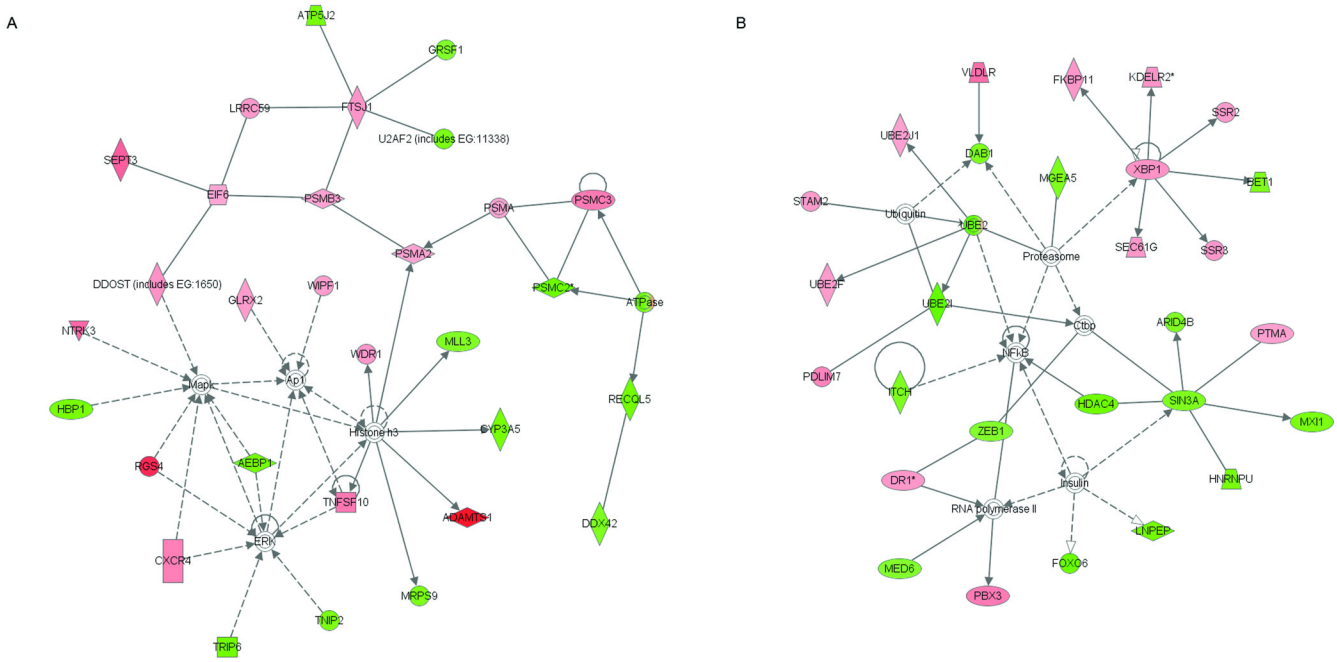

Figure 5.

Identification of highly significant networks of functional dependencies of genes from the top 300 del(7q) UL-specific gene list weighted for percent of del(7q) cells using Ingenuity Pathways Analysis. The functions of the two networks of highest significance are involved in (A) drug metabolism, organismal development and carbohydrate metabolism (score = 55, genes from deletion 7q list = 29) and (B) embryonic, nervous system and tissue development (score = 52, genes from deletion 7q list = 28). Pink shading indicates upregulated gene expression, green downregulated gene expression, solid lines a direct relationship between connected genes, and dotted lines an indirect relationship between linked genes.

Table 1

Histopathology, Karyotype, and FISH Results of Uterine Leiomyomata for del(7q) Study

Case Number	Accession Number	Sample Type	Histopathology	Karyotype	% del(7q)	Gene Expression Omnibus (GEO) Identifier[b]
1	ST91-026	del(7q) UL	--[a]	46,XX,del(7)(q22q32)[11]/46,XX[15]	42[d]	GSM321965
	ST91-027	Non-del(7q) UL	--	46,XX[9]	0[d]	GSM321966
	ST91-028	Myometrium	--	--	--	GSM321967
2	ST96-482	del(7q) UL	Usual type, low mitotic index	46,XX,del(7)(q22q32)[10]/46,XX[10]	50[d]	GSM321969
	ST96-481	Non-del(7q) UL	Usual type, low mitotic index	46,XX[20]	0[d]	GSM321968
	ST96-483	Myometrium	--	--	--	GSM321970
3	ST99-045	del(7q) UL	Usual type, low mitotic index	46,XX,del(7)(q22q32)[8]/46,XX[2]	80[d]	GSM321971
	ST99-047	Non-del(7q) UL	--	46,XX[8]	0[d]	GSM321972
	ST99-050	Myometrium	--	--	--	GSM321973
4	ST99-216	del(7q) UL	Cellular	46,XX,del(7)(q22q32)[13]	78[d]	GSM321974
	ST99-219	Non-del(7q) UL	Usual type, low mitotic index	46,XX[14]	0[d]	GSM321975
	ST99-220	Myometrium	--	--	--	GSM321976
5[c]	ST04-065	del(7q) UL	--	--	25% del(7q)/20% t(12;14)[e]	GSM321979
	ST04-066	Non-del(7q) UL	--	--	1% del(7q)/7% t(12;14)[ef]	GSM321978
	ST04-067	Myometrium	--	--	--	GSM321977
6	ST04-072F-2	del(7q) UL	Usual type with extensive hyalinization, low mitotic index	--	62[e]	GSM321981
	ST04-072F-1	Non-del(7q) UL	Usual type, low mitotic index	--	0[ef]	GSM321982
	ST04-072M	Myometrium	Normal myometrium	--	--	GSM321980
7	ST04-120F-2	del(7q) UL	Usual type, low mitotic index	--	52[e]	GSM321984
	ST04-120F-3	Non-del(7q) UL	--	--	0[ef]	GSM321985
	ST04-120M	Myometrium	--	--	--	GSM321983

Case Number	Accession Number	Sample Type	Histopathology	Karyotype	% del(7q)	Gene Expression Omnibus (GEO) Identifier[b]
8	ST05-004F-1	del(7q) UL	Usual type, low mitotic index	--	34[e]	GSM321988
	ST05-004F-2	Non-del(7q) UL	Usual type, low mitotic index	--	6[ef]	GSM321987
	ST05-004M	Myometrium	--	--	--	GSM321986
9	ST05-007F-4	del(7q) UL	Usual type, low mitotic index	--	37[e]	GSM321990
	ST05-007F-2	Non-del(7q) UL	Usual type, low mitotic index	--	5[ef]	GSM321991
	ST05-007M	Myometrium	--	--	--	GSM321989
10	ST05-024F-2	del(7q) UL	Usual type with extensive hyalinization, low mitotic index	--	12[e]	GSM321993
	ST05-024F-5	Non-del(7q) UL	Usual type, low mitotic index	--	5[ef]	GSM321994
	ST05-024M	Myometrium	--	--	--	GSM321992
11	ST05-025F-2	del(7q) UL	Usual type, low mitotic index	--	71[e]	GSM321995
	ST05-025F-4	Non-del(7q) UL	--	--	2[ef]	GSM321996
	ST05-025M	Myometrium	Normal myometrium	--	--	GSM321997

[a] Dash indicates unknown

[b] http://www.ncbi.nlm.nih.gov/geo/

[c] Case 5 involves a mosaic del(7q)(q22q32)/t(12;14)(q15;q23-q24) tumor

[d] Percentage of del(7q) cells determined by karyotype

[e] Percentage of del(7q) cells determined by FISH

[f] Value below FISH false positive cut-off for del(7q) of 9%

Table 2

Clinical Features of Uterine Leiomyomata with del(7q)

Case Number	Size of del(7q) Tumor (cm)	Size of Non-del(7q) Tumor (cm)	Total Number of Tumors	Race	Age of Onset (yrs)	Age at Surgery (yrs)	Menstrual Cycle[b]
1	_[a]	--	>5	White	48	48	Menstruation
2	14 × 10 × 9	3.5	2	Black	22	33	Secretory
3	6	5.5	5	Black	36	49	Menopausal
4	3	3.5	4	White	41	42	Proliferative
5	--	--	3	White	40	43	Menstruation
6	4 × 4 × 3.5	5.5 × 4.5 × 4.5	2	Hispanic	41	41	Secretory
7	6.5 × 5.5 × 5.2	2.1 × 1.8 × 1.6	3	White/Middle Eastern	41	45	Proliferative
8	10 × 7.5 × 6.5	9 × 5.5 × 5.5	36+	Black	43	45	Secretory
9	3.5 × 2.5 × 2	6.5 × 5.6 × 3.5	14	White	36	39	Menstruation
10	7 × 7 × 6	5 × 4 × 4	10	White	51	59	Menopausal
11	3.6 × 3.5 × 2.9	2.2 × 1.7 × 1.6	4	Black	39	51	Artificial Menopause (Megace-treated)

[a] Dash indicates unknown

[b] Based on day one of last menstrual period relative to surgery date (days 1–5=Menstruation; 6–14=Proliferative; 14–28+=Secretory; >100 days=Menopausal)

Table 3

Genes Downregulated in del(7q) UL Compared to Non-del(7q) UL

Number[a]	Probe Set	Ref Seq	Gene Symbol	Gene Title	Fold Change	P-value	Q-value	Chromosome
2	228138_at	NM_145115	ZNF498	zinc finger protein 498	−1.42	4.56E-05	0.337	7q22.1
3	1555363_s_at	XR_041448	MGC39821	hypothetical protein MGC39821	−1.67	4.90E-05	0.337	19p13.11
6	226100_at	NM_018682	MLL5	myeloid/lymphoid or mixed-lineage leukemia 5	−1.37	7.84E-05	0.337	7q22.2
8	238494_at	NM_015650	TRAF3IP1	TNF receptor-associated factor 3 interacting protein 1	−1.23	0.000149	0.492	2q37.3
9	200719_at	NM_006930	SKP1	S-phase kinase-associated protein 1	−1.19	0.000235	0.541	5q31.1
10	223384_s_at	NM_033017	TRIM4	tripartite motif-containing 4	−1.39	0.000304	0.541	7q22.1
12	233360_at	NM_003345	UBE2I	ubiquitin-conjugating enzyme E2I (UBC9 homolog, yeast)	−1.78	0.000377	0.541	16p13.3
13	226377_at	---	---	Transcribed locus	−1.3	0.000393	0.541	19p13.3
14	235634_at	NM_001015508	PURG	purine-rich element binding protein G	−1.45	0.00041	0.541	8p12
16	227983_at	NM_145058	RILPL2	Rab interacting lysosomal protein-like 2	−1.22	0.000437	0.541	12q24.31
23	226434_at	NM_145030	C7orf47	chromosome 7 open reading frame 47	−1.42	0.000653	0.541	7q22.1
25	1557038_s_at	---	---	Clone IMAGE:110862, mRNA sequence	−1.35	0.000744	0.541	13q32.3
26	1561539_at	---	---	CDNA clone IMAGE:5303543	−1.52	0.000801	0.541	11q14.2
27	218598_at	NM_021930	RINT1	RAD50 interactor 1	−1.43	0.000828	0.541	7q22.2
30	226040_at	---	---	MRNA; cDNA DKFZp762N156 (from clone DKFZp762N156)	−1.34	0.000887	0.541	7q22.1
31	223982_s_at	NM_015723	PNPLA8	patatin-like phospholipase domain containing 8	−1.27	0.000897	0.541	7q31.1
32	1553682_at	NM_152441	FBXL14	F-box and leucine-rich repeat protein 14	−1.54	0.000904	0.541	12p13.33
33	229321_s_at	---	---	CDNA FLJ35002 fis, clone OCBBF2011914	−1.27	0.000963	0.541	22q11.21
34	1554067_at	NM_152440	FLJ32549	hypothetical protein FLJ32549	−1.25	0.000975	0.541	12q14.2
35	200899_s_at	NM_012215	MGEA5	meningioma expressed antigen 5 (hyaluronidase)	−1.21	0.000984	0.541	10q24.32
36	218785_s_at	NM_022777	RABL5	RAB, member RAS oncogene family-like 5	−1.75	0.00102	0.541	7q22.1
37	238020_at	NM_002803	PSMC2	Proteasome (prosome, macropain) 26S subunit, ATPase, 2	−1.44	0.00102	0.541	7q22.1
38	236917_at	NM_153353	LRRC34	leucine rich repeat containing 34	−1.77	0.00103	0.541	3q26.2
40	225221_at	---	---	CDNA FLJ32068 fis, clone OCBBF1000114	−1.41	0.00103	0.541	7q22.1
42	225945_at	NM_001009958	ZNF655	zinc finger protein 655	−1.38	0.00104	0.541	7q22.1
43	204105_s_at	NM_001037132	NRCAM	neuronal cell adhesion molecule	−1.54	0.00104	0.541	7q31.1
44	213018_at	NM_021167	GATAD1	GATA zinc finger domain containing 1	−1.29	0.00108	0.541	7q21.2
45	233396_s_at	NM_020536	CSRP2BP	CSRP2 binding protein	−1.4	0.00111	0.541	20p11.23

Number[a]	Probe Set	Ref Seq	Gene Symbol	Gene Title	Fold Change	P-value	Q-value	Chromosome
46	213097_s_at	NM_014377	ZRF1	zuotin related factor 1	−1.43	0.00112	0.541	7q22.1
47	231436_at	---	---	Transcribed locus	−1.54	0.00122	0.541	15q13.3
52	38892_at	NM_015349	KIAA0240	KIAA0240	−1.24	0.00126	0.541	6p21.1
55	213154_s_at	NM_001003800	BICD2	bicaudal D homolog 2 (Drosophila)	−1.2	0.00138	0.541	9q22.31
56	244534_at	---	---	Transcribed locus	−1.56	0.00138	0.541	7q22.1
57	201788_at	NM_007372	DDX42	DEAD (Asp-Glu-Ala-Asp) box polypeptide 42	−1.19	0.00142	0.541	17q23.3
58	202054_s_at	NM_000382	ALDH3A2	aldehyde dehydrogenase 3 family, member A2	−1.34	0.00145	0.541	17p11.2
59	232454_at	---	---	MRNA; cDNA DKFZp586N2224 (from clone DKFZp586N2224)	−1.54	0.00146	0.541	9q34.13
60	1556409_a_at	XM_001725148	LOC100129932	hypothetical protein LOC100129932	−1.63	0.00148	0.541	11q21
61	231086_at	---	---	Transcribed locus	−1.2	0.00149	0.541	11q23.3
62	223424_s_at	NM_145914	ZSCAN21	zinc finger and SCAN domain containing 21	−1.31	0.00151	0.541	7q22.1
63	227899_at	NM_053276	VIT	vitrin	−1.6	0.00152	0.541	2p16.3
65	201068_s_at	NM_002803	PSMC2	proteasome (prosome, macropain) 26S subunit, ATPase, 2	−1.36	0.00156	0.541	7q22.1
69	222615_s_at	NM_024653	PRKRIP1	PRKR interacting protein 1 (IL11 inducible)	−1.38	0.00166	0.541	7q22.1
71	1559310_at	---	---	CDNA FLJ30875 fis, clone FEBRA2004331	−1.57	0.00168	0.541	9p13.3
73	210305_at	NM_001002810	PDE4DIP	phosphodiesterase 4D interacting protein (myomegalin)	−1.74	0.00169	0.541	1q21.1
75	233540_s_at	NM_001011649	CDK5RAP2	CDK5 regulatory subunit associated protein 2	−1.29	0.00172	0.541	9q33.2
76	1563797_at	---	---	CDNA FLJ23730 fis, clone HEP14530	−1.79	0.00176	0.541	6p12.1
77	209102_s_at	NM_012257	HBP1	HMG-box transcription factor 1	−1.29	0.00176	0.541	7q22.3
78	224873_s_at	NM_022497	MRPS25	mitochondrial ribosomal protein S25	−1.4	0.00177	0.541	3p24.3
80	227686_at	NM_138381	OXNAD1	oxidoreductase NAD-binding domain containing 1	−1.18	0.00179	0.541	3p24.3
81	242981_at	---	---	Transcribed locus	−1.3	0.00182	0.541	---
82	230619_at	NM_001668	ARNT	aryl hydrocarbon receptor nuclear translocator	−1.21	0.00186	0.541	1q21.2
83	240201_at	---	---	Transcribed locus	−1.36	0.00188	0.541	15q25.2
85	1554480_a_at	NM_031905	ARMC10	armadillo repeat containing 10	−1.58	0.00189	0.541	7q22.1
86	221192_x_at	NM_024311	MFSD11	major facilitator superfamily domain containing 11	−1.32	0.0019	0.541	17q25.2
89	1568874_at	NM_014071	NCOA6	nuclear receptor coactivator 6	−1.73	0.00192	0.541	20q11.22
90	202276_at	NM_006304	SHFM1	split hand/foot malformation (ectrodactyly) type 1	−1.29	0.00193	0.541	7q21.3-q22.1
94	230837_at	XR_041430	LOC647500	phosphodiesterase 4D interacting protein-like	−1.39	0.00203	0.541	1q21.1
95	227572_at	NM_032663	USP30	ubiquitin specific peptidase 30	−1.2	0.00209	0.541	12q24.11
96	218956_s_at	NM_015545	PTCD1	pentatricopeptide repeat domain 1	−1.57	0.00211	0.541	7q22.1

Number[a]	Probe Set	Ref Seq	Gene Symbol	Gene Title	Fold Change	P-value	Q-value	Chromosome
98	238076_at	NM_020699	GATAD2B	GATA zinc finger domain containing 2B	−1.45	0.00212	0.541	1q21.3
99	225136_at	NM_021623	PLEKHA2	pleckstrin homology domain containing, family A member 2	−1.16	0.00214	0.541	8p11.23

[a]Genes are those in the top 100 del(7q) UL-specific list (a more extensive list can be found as an online supplement)

Table 4

Genes Upregulated in del(7q) UL Compared to Non-del(7q) UL

Number[a]	Probe Set	Ref Seq	Gene Symbol	Gene Title	Fold Change	P-value	Q-value	Chromosome
1	200652_at	NM_003145	SSR2	signal sequence receptor, beta (translocon-associated protein beta)	1.26	3.99E-05	0.337	1q22
4	225897_at	NM_002356	MARCKS	myristoylated alanine-rich protein kinase C substrate	1.32	5.29E-05	0.337	6q22.1
5	212552_at	NM_002149	HPCAL1	hippocalcin-like 1	1.47	7.43E-05	0.337	2p25.1
7	204360_s_at	NM_000263	NAGLU	N-acetylglucosaminidase, alpha- (Sanfilippo disease IIIB)	1.33	8.94E-05	0.337	17q21.31
11	225065_x_at	NM_152350	C17orf45	chromosome 17 open reading frame 45	1.89	0.000367	0.541	17p11.2
15	200052_s_at	NM_004515	ILF2	interleukin enhancer binding factor 2, 45kDa	1.26	0.000412	0.541	1q21.3
17	211852_s_at	NM_139321	ATRN	attractin	1.66	0.000443	0.541	20p13
18	200700_s_at	NM_001100603	KDELR2	KDEL (Lys-Asp-Glu-Leu) endoplasmic reticulum protein retention receptor 2	1.36	0.000457	0.541	7p22.1
19	201317_s_at	NM_002787	PSMA2	proteasome (prosome, macropain) subunit, alpha type, 2	1.15	0.000459	0.541	7p14.1
20	214108_at	NM_002382	MAX	MYC associated factor X	1.49	0.000487	0.541	14q23.3
21	207998_s_at	NM_000720	CACNA1D	calcium channel, voltage-dependent, L type, alpha 1D subunit	1.82	0.000574	0.541	3p21.1
22	235290_at	NM_001001662	ZNF782	Zinc finger protein 782	1.28	0.000582	0.541	9q22.33
24	226390_at	NM_139164	STARD4	StAR-related lipid transfer (START) domain containing 4	1.64	0.000654	0.541	5q22.1
28	223241_at	NM_013321	SNX8	sorting nexin 8	1.69	0.000853	0.541	7p22.2
29	233419_at	---	---	CDNA FLJ11851 fis, clone HEMBA1006744	2.2	0.000856	0.541	9p24.2
39	242707_at	NM_004830	MED23	mediator complex subunit 23	1.93	0.00103	0.541	6q23.2
41	211864_s_at	NM_013451	FER1L3	fer-1-like 3, myoferlin (C. elegans)	1.51	0.00103	0.541	10q23.33
48	204095_s_at	NM_006532	ELL	elongation factor RNA polymerase II	1.45	0.00122	0.541	19p13.11
49	223614_at	---	C8orf57	chromosome 8 open reading frame 57	1.74	0.00124	0.541	8q21.3
50	208708_x_at	NM_001969	EIF5	eukaryotic translation initiation factor 5	1.21	0.00124	0.541	14q32.32
51	217771_at	NM_016548	GOLM1	golgi membrane protein 1	1.42	0.00126	0.541	9q21.33
53	210868_s_at	NM_024090	ELOVL6	ELOVL family member 6, elongation of long chain fatty acids	1.46	0.00135	0.541	4q25
54	212121_at	NM_015631	TCTN3	tectonic family member 3	1.18	0.00135	0.541	10q23.33
64	201267_s_at	NM_002804	PSMC3	proteasome (prosome, macropain) 26S subunit, ATPase, 3	1.67	0.00155	0.541	11p11.2
66	204082_at	NM_006195	PBX3	pre-B-cell leukemia homeobox 3	1.66	0.00157	0.541	9q33.3
67	209188_x_at	NM_001938	DR1	down-regulator of transcription 1, TBP-binding (negative cofactor 2)	1.32	0.0016	0.541	1p22.1
68	202687_s_at	NM_003810	TNFSF10	tumor necrosis factor (ligand) superfamily, member 10	1.7	0.00163	0.541	3q26.31
70	219118_at	NM_016594	FKBP11	FK506 binding protein 11, 19 kDa	1.33	0.00166	0.541	12q13.12

Number[a]	Probe Set	Ref Seq	Gene Symbol	Gene Title	Fold Change	P-value	Q-value	Chromosome
72	218384_at	NM_001042476	CARHSP1	calcium regulated heat stable protein 1, 24kDa	1.76	0.00169	0.541	16p13.2
74	231948_s_at	NM_080678	UBE2F	ubiquitin-conjugating enzyme E2F (putative)	1.27	0.00171	0.541	2q37.3
79	200670_at	NM_001079539	XBP1	X-box binding protein 1	1.38	0.00178	0.541	22q12.1
84	200754_x_at	NM_003016	SFRS2	splicing factor, arginine/serine-rich 2	1.23	0.00189	0.541	17q25.2
87	243159_x_at	---	---	Transcribed locus	15.9[b]	0.0019	0.541	5p15.1
88	200753_x_at	NM_003016	SFRS2	splicing factor, arginine/serine-rich 2	1.31	0.00192	0.541	17q25.2
91	205499_at	NM_014467	SRPX2	sushi-repeat-containing protein, X-linked 2	2.02	0.00197	0.541	Xq22.1
92	1555928_at	---	---	CDNA FLJ30680 fis, clone FCBBF2000123	4.83	0.00199	0.541	---
93	228061_at	NM_138771	CCDC126	coiled-coil domain containing 126	1.65	0.002	0.541	7p15.3
97	216697_at	NM_007118	TRIO	Triple functional domain (PTPRF interacting)	2.47	0.00212	0.541	5p15.2
100	1558996_at	NM_001012505	FOXP1	forkhead box P1	1.5	0.00219	0.541	3p14.1

[a] Genes are those in the top 100 del(7q) UL-specific list (a more extensive list can be found as an online supplement)

[b] Removal of a single patient outlier for this probe set reduces the fold change to 3.9.

Table 5

Genes Upregulated or Downregulated in del(7q) UL Compared to Non-del(7q) UL Weighted for Percent Mosaicism

Number[a]	Non-weighted[b]	Probe Set	Ref Seq	Gene Symbol	Gene Title	Fold Change	P-value	Q-value	Chromosome
1	2	228138_at	NM_145115	ZNF498	zinc finger protein 498	−1.42	9.56E-07	0.0239	7q22.1
2	8	238494_at	NM_015650	TRAF3IP1	TNF receptor-associated factor 3 interacting protein 1	−1.23	9.49E-06	0.0753	2q37.3
3	3	1555363_s_at	XR_041448	MGC39821	hypothetical protein MGC39821	−1.67	1.23E-05	0.0753	19p13.11
4	6	226100_at	NM_018682	MLL5	myeloid/lymphoid or mixed-lineage leukemia 5	−1.37	1.48E-05	0.0753	7q22.2
5	1	200652_at	NM_003145	SSR2	signal sequence receptor, beta (translocon-associated protein beta)	1.26	1.52E-05	0.0753	1q22
6	4	225897_at	NM_002356	MARCKS	myristoylated alanine-rich protein kinase C substrate	1.32	1.81E-05	0.0753	6q22.1
7	77	209102_s_at	NM_012257	HBP1	HMG-box transcription factor 1	−1.29	2.96E-05	0.106	7q22.3
8	17	211852_s_at	NM_139321	ATRN	attractin	1.66	8.79E-05	0.207	20p13
9	175	214670_at	NM_003439	ZKSCAN1	zinc finger with KRAB and SCAN domains 1	−1.46	8.90E-05	0.207	7q22.1
10	9	200719_at	NM_006930	SKP1	S-phase kinase-associated protein 1	−1.19	9.40E-05	0.207	5q31.1
11	10	223384_s_at	NM_033017	TRIM4	tripartite motif-containing 4	−1.39	9.50E-05	0.207	7q22.1
12	62	223424_s_at	NM_145914	ZSCAN21	zinc finger and SCAN domain containing 21	−1.31	9.94E-05	0.207	7q22.1
13	7	204360_s_at	NM_000263	NAGLU	N-acetylglucosaminidase, alpha- (Sanfilippo disease IIIB)	1.33	0.000128	0.225	17q21.31
14	37	238020_at	NM_002803	PSMC2	Proteasome (prosome, macropain) 26S subunit, ATPase, 2	−1.44	0.000132	0.225	7q22.1
15	42	225945_at	NM_001009958	ZNF655	zinc finger protein 655	−1.38	0.000151	0.225	7q22.1
16	23	226434_at	NM_145030	C7orf47	chromosome 7 open reading frame 47	−1.42	0.000164	0.225	7q22.1
17	11	225065_x_at	NM_152350	C17orf45	chromosome 17 open reading frame 45	1.89	0.000168	0.225	17p11.2
18	5	212552_at	NM_002149	HPCAL1	hippocalcin-like 1	1.47	0.000176	0.225	2p25.1
19	46	213097_s_at	NM_014377	ZRF1	zuotin related factor 1	−1.43	0.000176	0.225	7q22.1
20	95	227572_at	NM_032663	USP30	ubiquitin specific peptidase 30	−1.2	0.00018	0.225	12q24.11
21	16	227983_at	NM_145058	RILPL2	Rab interacting lysosomal protein-like 2	−1.22	0.000191	0.228	12q24.31
22	19	201317_s_at	NM_002787	PSMA2	proteasome (prosome, macropain) subunit, alpha type, 2	1.15	0.00021	0.235	7p14.1
23	40	225221_at	---	---	CDNA FLJ32068 fis, clone OCBBF1000114	−1.41	0.000241	0.235	7q22.1
24	180	201405_s_at	NM_006833	COPS6	COP9 constitutive photomorphogenic homolog subunit 6 (Arabidopsis)	−1.34	0.000243	0.235	7q22.1
25	553	219155_at	NM_012417	PITPNC1	phosphatidylinositol transfer protein, cytoplasmic 1	1.52	0.000249	0.235	17q24.2
26	179	221998_s_at	NM_001025778	VRK3	vaccinia related kinase 3	−1.24	0.000253	0.235	19q13.33
27	14	235634_at	NM_001015508	PURG	purine-rich element binding protein G	−1.45	0.000254	0.235	8p12
28	34	1554067_at	NM_152440	FLJ32549	hypothetical protein FLJ32549	−1.25	0.000294	0.249	12q14.2

Number[a]	Non-weighted[b]	Probe Set	Ref Seq	Gene Symbol	Gene Title	Fold Change	P-value	Q-value	Chromosome
29	153	201682_at	NM_004279	PMPCB	peptidase (mitochondrial processing) beta	−1.38	3.00E-04	0.249	7q22.1
30	81	242981_at	---	---	Transcribed locus	−1.3	0.000303	0.249	---
31	56	244534_at	---	---	Transcribed locus	−1.56	0.00031	0.249	7q22.1
32	107	208808_s_at	NM_002129	HMGB2	high-mobility group box 2	−1.26	0.000318	0.249	4q34.1
33	13	226377_at	---	---	Transcribed locus	−1.3	0.000341	0.258	19p13.3
34	43	204105_s_at	NM_001037132	NRCAM	neuronal cell adhesion molecule	−1.54	0.000366	0.258	7q31.1
35	31	223982_s_at	NM_015723	PNPLA8	patatin-like phospholipase domain containing 8	−1.27	0.000377	0.258	7q31.1
36	44	213018_at	NM_021167	GATAD1	GATA zinc finger domain containing 1	−1.29	0.000388	0.258	7q21.2-q22
37	130	228346_at	---	---	Transcribed locus	−1.22	0.000395	0.258	19p13.2
38	55	213154_s_at	NM_001003800	BICD2	bicaudal D homolog 2 (Drosophila)	−1.2	0.000399	0.258	9q22.31
39	96	218956_s_at	NM_015545	PTCD1	pentatricopeptide repeat domain 1	−1.57	0.000403	0.258	7q22.1
40	27	218598_at	NM_021930	RINT1	RAD50 interactor 1	−1.43	0.000437	0.266	7q22.2
41	18	200700_s_at	NM_001100603	KDELR2	KDEL (Lys-Asp-Glu-Leu) endoplasmic reticulum protein retention receptor 2	1.36	0.000445	0.266	7p22.1
42	57	201788_at	NM_007372	DDX42	DEAD (Asp-Glu-Ala-Asp) box polypeptide 42	−1.19	0.000457	0.266	17q23.3
43	168	227187_at	---	---	Transcribed locus	−1.34	0.000457	0.266	7q31.1
44	158	1569077_x_at	NM_001102657	FLJ16287	FLJ16287 protein	−1.34	0.000481	0.266	19q13.33
45	91	205499_at	NM_014467	SRPX2	sushi-repeat-containing protein, X-linked 2	2.02	0.000494	0.266	Xq22.1
46	133	203484_at	NM_001012456	SEC61G	Sec61 gamma subunit	1.31	0.000515	0.266	7p11.2
47	114	206659_at	XR_041868	FLJ14082	hypothetical protein FLJ14082	−1.39	0.000524	0.266	2q11.1
48	85	1554480_a_at	NM_031905	ARMC10	armadillo repeat containing 10	−1.58	0.000531	0.266	7q22.1
49	159	242621_at	NM_145115	ZNF498	zinc finger protein 498	−1.34	0.00054	0.266	7q22.1
50	90	202276_at	NM_006304	SHFM1	split hand/foot malformation (ectrodactyly) type 1	−1.29	0.000541	0.266	7q21.3-q22.1

[a] Genes are those in the top 50 del(7q) UL-specific list that have been weighted for the percent mosaicism (a more extensive list can be found as an online supplement)

[b] Number on non-weighted del(7q) UL-specific gene list

Table 6

Genes in the aCGH-defined Smallest Commonly Deleted Region on 7q with Significant ($p < 0.01$) Expression in del(7q) UL Relative to Non-del(7q) UL

Probe Set	Ref Seq	Gene Symbol	Gene Title	Fold Change[a]	Chromosome
205690_s_at	NM_003910	BUD31	BUD31 homolog (S. cerevisiae)	−0.567	7q22.1
218956_s_at	NM_015545	PTCD1	pentatricopeptide repeat domain 1	−1.05	7q22.1
206688_s_at	NM_001081559	CPSF4	cleavage and polyadenylation specific factor 4, 30kDa	−0.529	7q22.1
202961_s_at	NM_001003713	ATP5J2	ATP synthase, H+ transporting, mitochondrial F0 complex, subunit F2	−0.379	7q22.1
214714_at	NM_032164	ZNF394	zinc finger protein 394	−0.541	7q22.1
203730_s_at	NM_014569	ZKSCAN5	zinc finger with KRAB and SCAN domains 5	−0.544	7q22.1
225945_at	NM_001009958	ZNF655	zinc finger protein 655	−0.624	7q22.1
242621_at; 228138_at	NM_145115	ZNF498	zinc finger protein 498	−0.584; −0.602	7q22.1
205765_at; 214235_at	NM_000777	CYP3A5	cytochrome P450, family 3, subfamily A, polypeptide 5	−1.79; −0.956	7q22.1
223384_s_at; 1554287_at	NM_033017	TRIM4	tripartite motif-containing 4	−0.558; −0.941	7q22.1
214670_at; 1557953_at	NM_003439	ZKSCAN1	zinc finger with KRAB and SCAN domains 1	−0.83; −0.869	7q22.1
225221_at	---	GATS	opposite strand transcription unit to STAG3	−0.593	7q22.1
223424_s_at	NM_145914	ZSCAN21	zinc finger and SCAN domain containing 21	−0.503	7q22.1
232497_at	NM_017715	ZNF3	zinc finger protein 3	−1.4	7q22.1
201405_s_at; 213504_at	NM_006833	COPS6	COP9 constitutive photomorphogenic homolog subunit 6 (Arabidopsis)	−0.555; −0.479	7q22.1
210983_s_at	NM_005916	MCM7	minichromosome maintenance complex component 7	−0.495	7q22.1
227313_at	NM_152755	CNPY4	canopy 4 homolog (zebrafish)	−0.669	7q22.1
224890_s_at	NM_001008395	LOC389541	similar to CG14977-PA	−0.457	7q22.1
225321_s_at; 220954_s_at	NM_013440	PILRB	paired immunoglobin-like type 2 receptor beta	−0.694; −0.573	7q22.1
220618_s_at	NM_017984	ZCWPW1	zinc finger, CW type with PWWP domain 1	−0.679	7q22.1
219798_s_at	NM_019606	MEPCE	methylphosphate capping enzyme	−0.529	7q22.1
226434_at	NM_145030	C7orf47	chromosome 7 open reading frame 47	−0.577	7q22.1
209482_at	NM_005837	POP7	processing of precursor 7, ribonuclease P/MRP subunit (S. cerevisiae)	−0.482	7q22.1
209129_at	NM_003302	TRIP6	thyroid hormone receptor interactor 6	−0.569	7q22.1
214808_at	---	---	---	−0.56	7q22.1
226040_at	---	---	---	−0.489	7q22.1
222742_s_at; 218785_s_at	NM_022777	RABL5	RAB, member RAS oncogene family-like 5	−0.645; −0.929	7q22.1
218378_s_at; 222615_s_at	NM_024653	PRKRIP1	PRKR interacting protein 1 (IL11 inducible)	−0.816; −0.553	7q22.1

Probe Set	Ref Seq	Gene Symbol	Gene Title	Fold Change[a]	Chromosome
212706_at; 208534_s_at	NM_001079877	RASA4	RAS p21 protein activator 4	−0.661; −0.805	7q22.1
1554480_a_at; 223328_at	NM_031905	ARMC10	armadillo repeat containing 10	−0.829; −0.589	7q22.1
226041_at; 242229_at	NM_001122838	NAPEPLD	N-acyl phosphatidylethanolamine phospholipase D	−0.617; −0.477	7q22.1
201682_at	NM_004279	PMPCB	peptidase (mitochondrial processing) beta	−0.654	7q22.1
213097_s_at	NM_014377	ZRF1	zuotin related factor 1	−0.623	7q22.1
244534_at	---	RELN	reelin	−0.685	7q22.1
201067_at; 238020_at	NM_002803	PSMC2	proteasome (prosome, macropain) 26S subunit, ATPase, 2	−0.537; −0.593	7q22.1
204957_at	NM_002553	ORC5L	origin recognition complex, subunit 5-like (yeast)	−0.652	7q22.2
236761_at	NM_199000	LHFPL3	lipoma HMGIC fusion partner-like 3	1.82	7q22.2-q22.3
226100_at	NM_018682	MLL5	myeloid/lymphoid or mixed-lineage leukemia 5	−0.54	7q22.3
230091_at; 203181_x_at; 203182_s_at	---	SRPK2	SFRS protein kinase 2	−0.848; −0.743; −0.789	7q22.3
218984_at	NM_019042	PUS7	pseudouridylate synthase 7 homolog (S. cerevisiae)	−0.642	7q22.3
218598_at	NM_021930	RINT1	RAD50 interactor 1	−0.594	7q22.3
209102_s_at	NM_012257	HBP1	HMG-box transcription factor 1	−0.499	7q22.3
203629_s_at; 203630_s_at	NM_006348	COG5	component of oligomeric golgi complex 5	−0.721; −0.629	7q22.3
205761_s_at; 205762_s_at	NM_181581	DUS4L	dihydrouridine synthase 4-like (S. cerevisiae)	−0.718; −0.989	7q22.3
225674_at; 225677_at; 217657_at	NM_001008405	BCAP29	B-cell receptor-associated protein 29	−0.604; −0.618; −0.716	7q22.3
227187_at	---	LAMB1	laminin, beta 1	−0.578	7q31.1
209095_at	NM_000108	DLD	dihydrolipoamide dehydrogenase	−0.655	7q31.1
236437_at	---	LAMB4	laminin beta 4	−0.856	7q31.1
204105_s_at	NM_001037132	NRCAM	neuronal cell adhesion molecule	−0.84	7q31.1
223310_x_at; 223982_s_at	NM_015723	PNPLA8	patatin-like phospholipase domain containing 8	−0.43; −0.399	7q31.1
227636_at	NM_182529	THAP5	THAP domain containing 5	−0.57	7q31.1

[a]Expression is the $\log_2$(fold change) between del(7q) UL relative to non-del(7q) UL weighted for percent of del(7q) cell mosaicism